Erosion Susceptibility in the area Around the Okanogan Fire Complex, Washington, US

1. Problem

Construct a raster that represents susceptibility to erosion based on lithology, slope, cover type, burned area, and precipitation in the area in and around the Okanogan Fire Complex.

2. Methods

2.1 Data Collection

2.1.1 Burned Area

The Okanogan Fire Complex was chosen for this study because it is a recent (September 22nd, 2015), large fire in relatively rough topography with many lithologies, and various vegetation cover types. The shapefile for the full extent of the fire was found on USGS's website under Geosciences and Environmental Change Science Center (GECSC) Outgoing datasets. The original shape file was projected using the USA Contiguous Albers Equal Area Conic USGS Version Projection with the 1983 North American Datum.

2.1.2 Geology

The Geology shapefiles, including lithology and structure, where acquired from the Washington State Department of Natural Resources under GIS Data and Databases. The Geologic data I used was from the surface geology section at a 1:100,000 scale. The file is a geodatabase with classes including, geology, folds, and faults, the three feature classes used in my project. The data was originally projected on 1983 North American Datum HARN State Plane Washington South FIPS 4602 Feet.

2.1.3 National Elevation Dataset

The elevation used to make a slope raster is made up of two tiles from the National Elevation Dataset at 1/3 arc-second resolution. The data was collected from the USGS National Map Download. It was based on the horizontal 1983 North American Datum and the North American Vertical Datum of 1988. The elevation is in meters.

2.1.4 National Agriculture Imagery Program

The imagery data was from the National Agriculture Imagery Program (NAIP) collected from the USGS National Map Download. The imagery is made of 3.75 by 3.75 minute at 1 meter resolution. The imagery data was taken in 2013 so the groundcover data is from before the fires. The data is formatted using the 1983 North American Datum.

2.1.5 Transportation

The transportation shapefiles were also from the USGS National Map Download. They used the 1983 North American Datum. The transportation information included shape files for roads.

2.1.6 Hydrography

The hydrography data was collected from the Washington State Department of Natural Resource's website from their Available GIS Data page. The hydrography data included shapefiles for lines and polygons which contained information pertaining to stream, lake, and other water feature's locations. The files were projected, originally, using the 1983 North American Datum State Plane Washington South FIPS 4602 feet.

2.1.7 Precipitation

The precipitation data is from PRISM Climate Group North Alliance for Computational Science and Engineering. The data is projected using the 1983 North American Datum. The

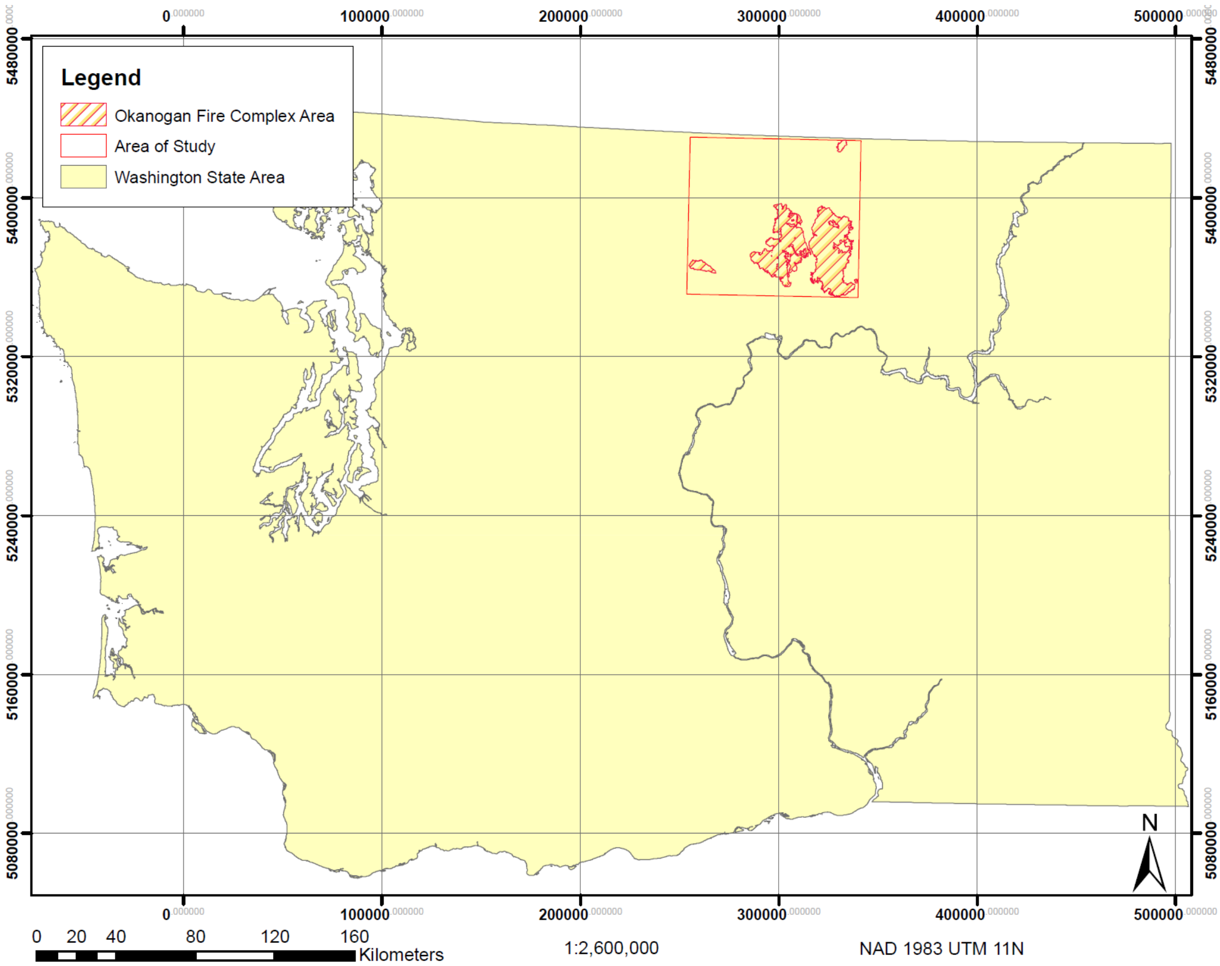

Figure 1: Map of analysis area in red with the location in Washington and the burn extent.

data is annual precipitation values for 30 year normals for a period from 1981 to 2010. The data is in units of millimeters.

2.2 Data Management

2.2.1 Shapefiles

The burn area, geology, transportation, and hydrography shapefiles were projected using the project tool to 1983 NAD with UTM coordinates. Then the data was clipped to the boundary area.

2.2.2 Raster Data

The raster data was slightly more involved because multiple tiles for imagery and elevation were needed to cover the entire analysis area.

The imagery data is made up of over 250 3.75 by 3.75 minute tiles at 1 meter scale. The data was mosaicked together using the mosaic tool, then projected using the project raster tool, and then resampled with a cell size of 5 m. A cell size of 5 m was chosen because that was the lowest resolution at which individual large trees were distinguishable. This capability would be needed when creating a cover type raster. After the raster had been mosaicked, projected, and resampled, it was clipped to the boundary using the clip tool.

FID	LITHOLOGY	Rank
0	acidic (felsic) intrusive rocks	2
1	alkalic intrusive rocks	2
2	alluvium	13
3	alluvium, older (includes alluvial fans and talus)	12
4	amphibolite	2
5	andesite flows	4
6	banded gneiss	2
7	basalt flows (GrandeRondeBasalt,upper flows of norm.mag.pol.)	4
8	basic (mafic) intrusive rocks	2
9	calc-silicate rock	6
10	continental glacial drift, Fraser-age	14
11	continental glacial outwash, Fraser-age	14
12	continental glacial till, Fraser-age	14
13	continental sedimentary deposits or rocks	9
14	continental sedimentary deposits or rocks, conglomerate	6
15	dacite flows	4
16	diorite	2
17	dune sand	15
18	gabbro	2
19	glaciolacustrine deposits, Fraser-age	14
20	gneiss	2
21	granite	2
22	granodiorite	2
23	heterogeneous metamorphic rocks	3
24	intermediate intrusive rocks	2
25	intrusive andesite	2
26	intrusive dacite	2
27	intrusive rocks, undivided	2
28	marble	7
29	marine metasedimentary rocks	8
30	marine sedimentary rocks	9
31	mass-wasting deposits, mostly landslides	16
32	metacarbonate	3
33	metasedimentary and metavolcanic rocks	2
34	metavolcanic rocks	2
35	migmatite	2
36	mixed metamorphic and igneous rocks	2
37	monzodiorite	2
38	orthogneiss	2
39	orthogneiss, mesocratic	2
40	peat deposits	12
41	quartz diorite	2
42	quartz monzonite	2
43	quartzite, high grade	1
44	sedimentary deposits or rocks	6
45	sedimentary deposits or rocks, undivided	6
46	tectonic breccia	11
47	tectonic zone	11
48	tonalite	4
49	tuffs and tuff breccias	11
50	ultrabasic (ultramafic) rocks	6
51	volcanic and sedimentary rocks	5
52	volcanic rocks	4
53	volcanic rocks, undivided	4
54	volcaniclastic deposits or rocks	10
55	water	0

Table 1: Table of lithology ranks. Ranks of lithologies were based roughly on experimental data determining the strength of different lithologies in Sklar and Dietrich (2001).

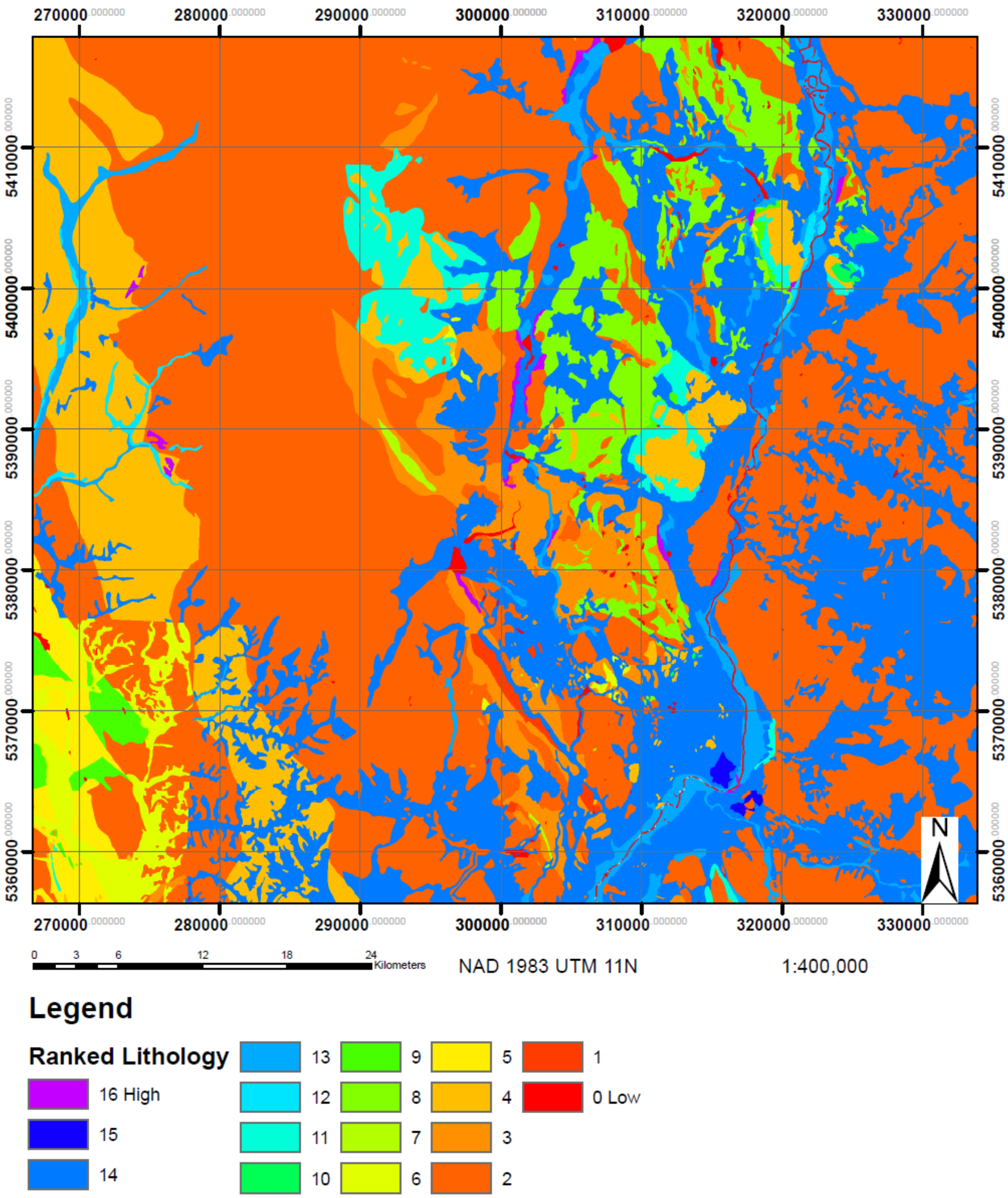

Figure 2: Map of the ranked geology raster. Red are the hardest lithologies to erode and purple are the easiest.

The elevation data is made up of two 1/3 arc-second tiles. These were mosaicked, projected, and resampled using the same methods as discussed in the imagery section. This data was then clipped to the boundary.

The precipitation data was for the entire US and therefore did not need to be mosaicked. The data was first projected, and then resampled at a cell size of 5 m. Then it was clipped to the boundary.

2.3 Constructing Ranked Rasters

2.3.1 Geology Rank

The geology polygon layer file was used to first create a dissolved geology shapefile based on lithology. This resulted in 56 different types of lithology. This dissolved layer file was then rasterized at 5 m cell size. After the raster was created, it was reclassified using Table 1. Ranks were based on experimentally determined strengths of lithologies from Sklar and Deitrich (2001). The resulting ranked raster is in Figure 2.

2.3.2 Cover Type and Fire Rank

The cover type raster was created by using the image classification toolbar to classify the imagery data based on 5 determined cover types, mixed vegetation, grass, trees, water, and barren land. The image was classified using the maximum likelihood classification tool based on a signature file created from the chosen areas in Figure 3. The cover type raster from this classification is in Figure 4. The cover type was then ranked based on the relative strengths of mixed vegetation, grass, trees, and barren land using Reubens and others (2006). I determined values to be -12, -8, -4, 0, and 4 for mixed vegetation, grass, trees, water, and barren land, respectively. The specific numbers were based on trying to balance the effects of lithology and cover type. By assigning negative values to vegetation types,

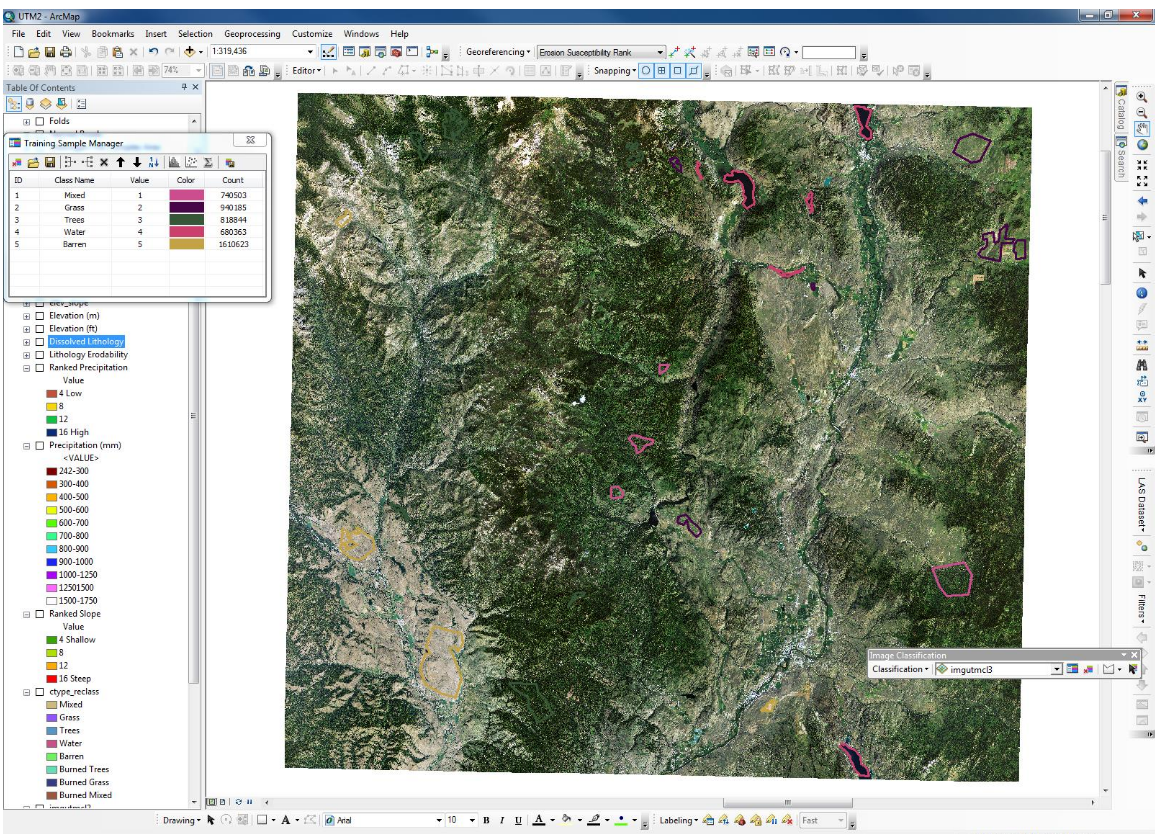

Figure 3: A screen shot of ArcMap with areas that were selected to use for classifying the image based on cover type. The key for colored regions and labels is in the upper left corner.

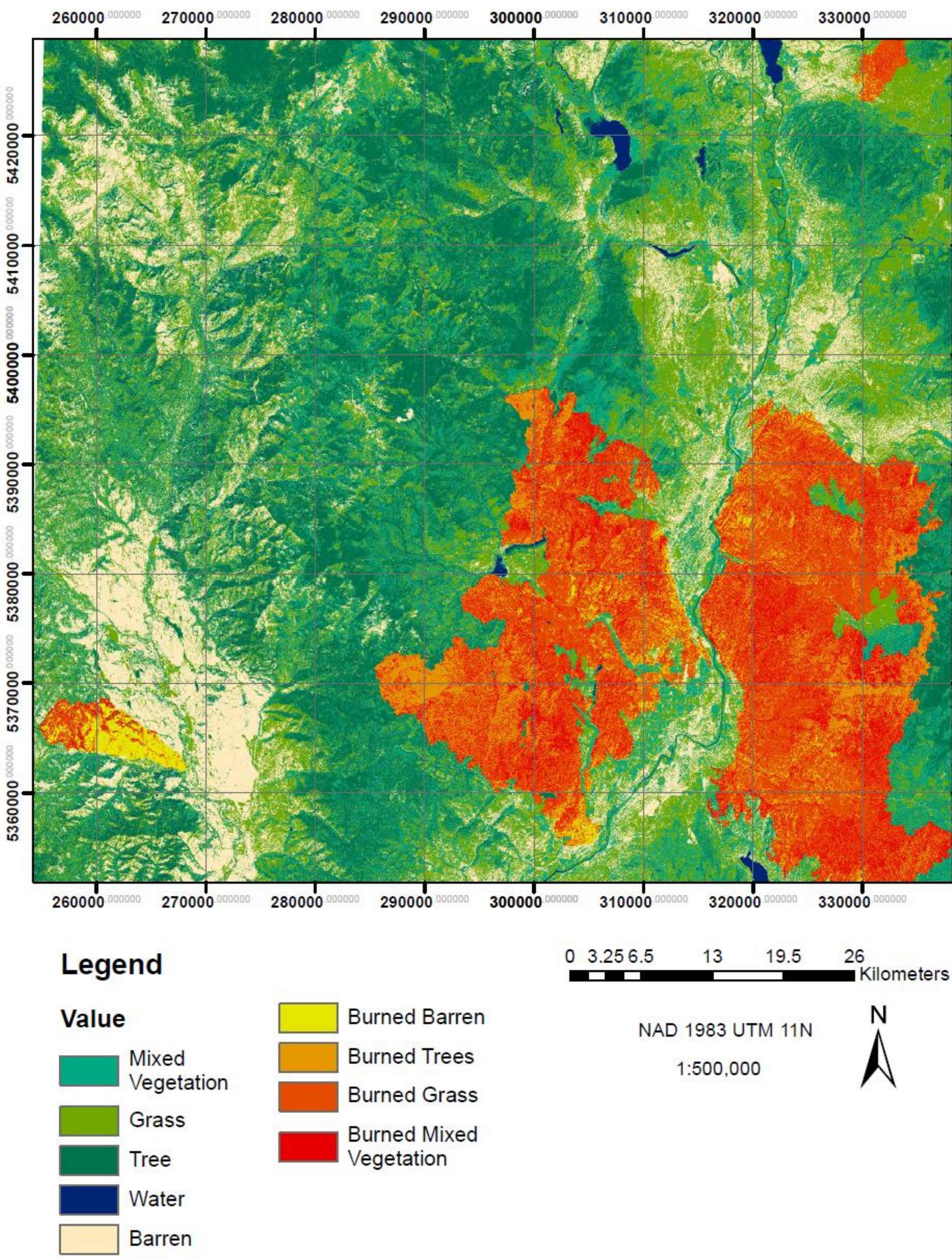

Figure 5: Map of the ranked cover type raster with burned cover. This is the cover type raster used to calculate the erosion susceptibility map

because, in reality vegetation, would stabilize the slope and therefore decrease erosion susceptibility. In order to complete the cover type rank, I had to incorporate the effects of burned vegetation into the ranked raster. This was done by adding the converted fire raster which had values of 0 for no fire and 1 for fire to the cover type raster. This would result in a raster with values of -12, -11, -8, -7, -4, -3, 0, 1, 4, and 5 for mixed vegetation, burned mixed vegetation, grass, burned grass, trees, burned trees, water, burned water, barren land, and burned barren land, respectively. The raster was then reclassified to its final rank of -12, -8, -4, 0, 4, 6, 8, 12, and 16 for mixed vegetation, grass, trees, water, barren land, burned barren land, burned trees, burned grass, and burned mixed vegetation, respectively. The map of the ranked cover type is shown in Figure 5.

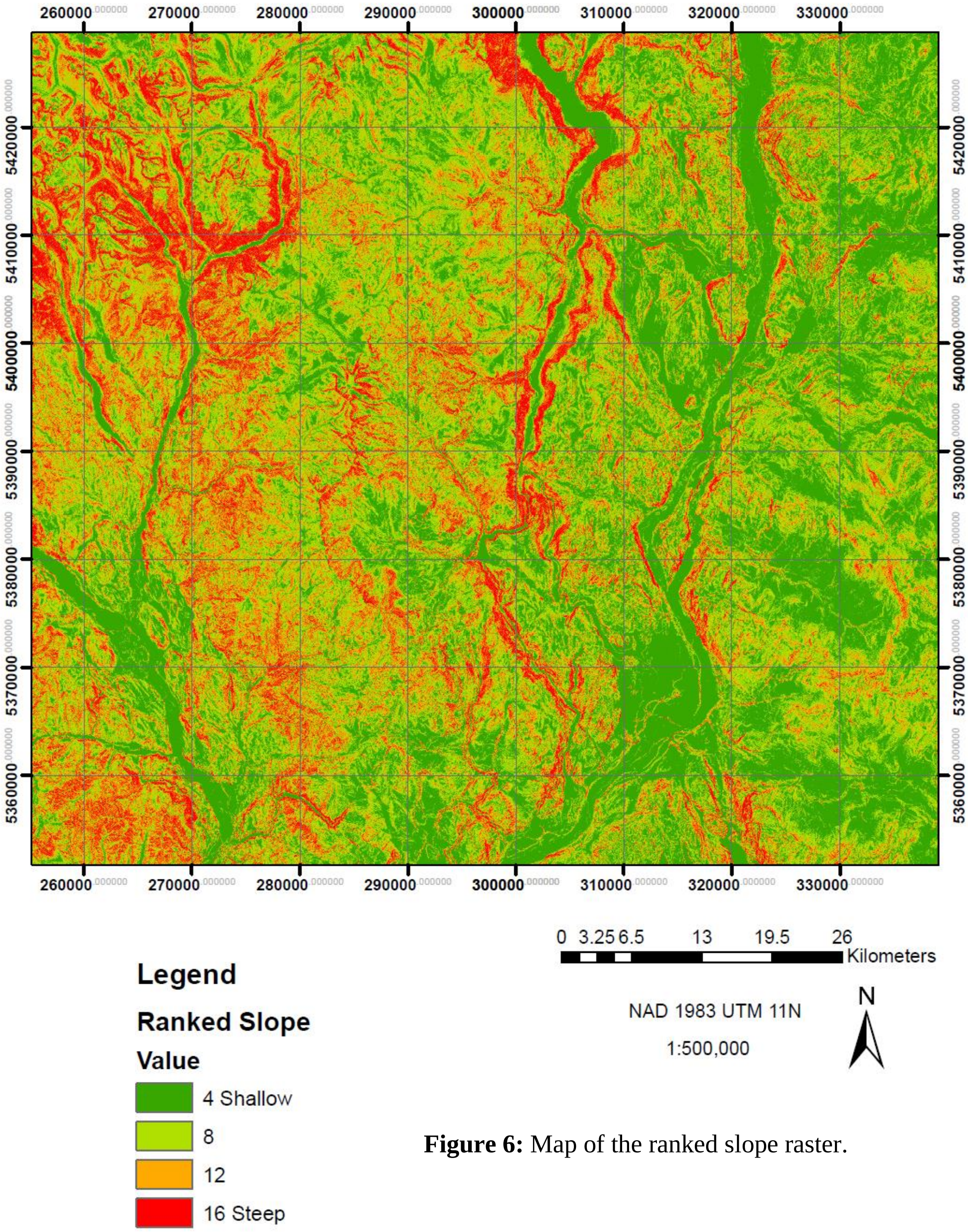

Figure 6: Map of the ranked slope raster.

2.3.3 Ranked Slope Raster

The ranked slope raster was created using the elevation raster made from NED data. The slope raster was calculated from the elevation raster using the slope tool. The slope was then ranked using a similar breakdown to the one from lab 11. However, the rank breakdown was scaled up to match the easiest erodible lithology and cover type. The resulting ranked raster is in Figure 6.

2.3.4 Precipitation Ranked Raster

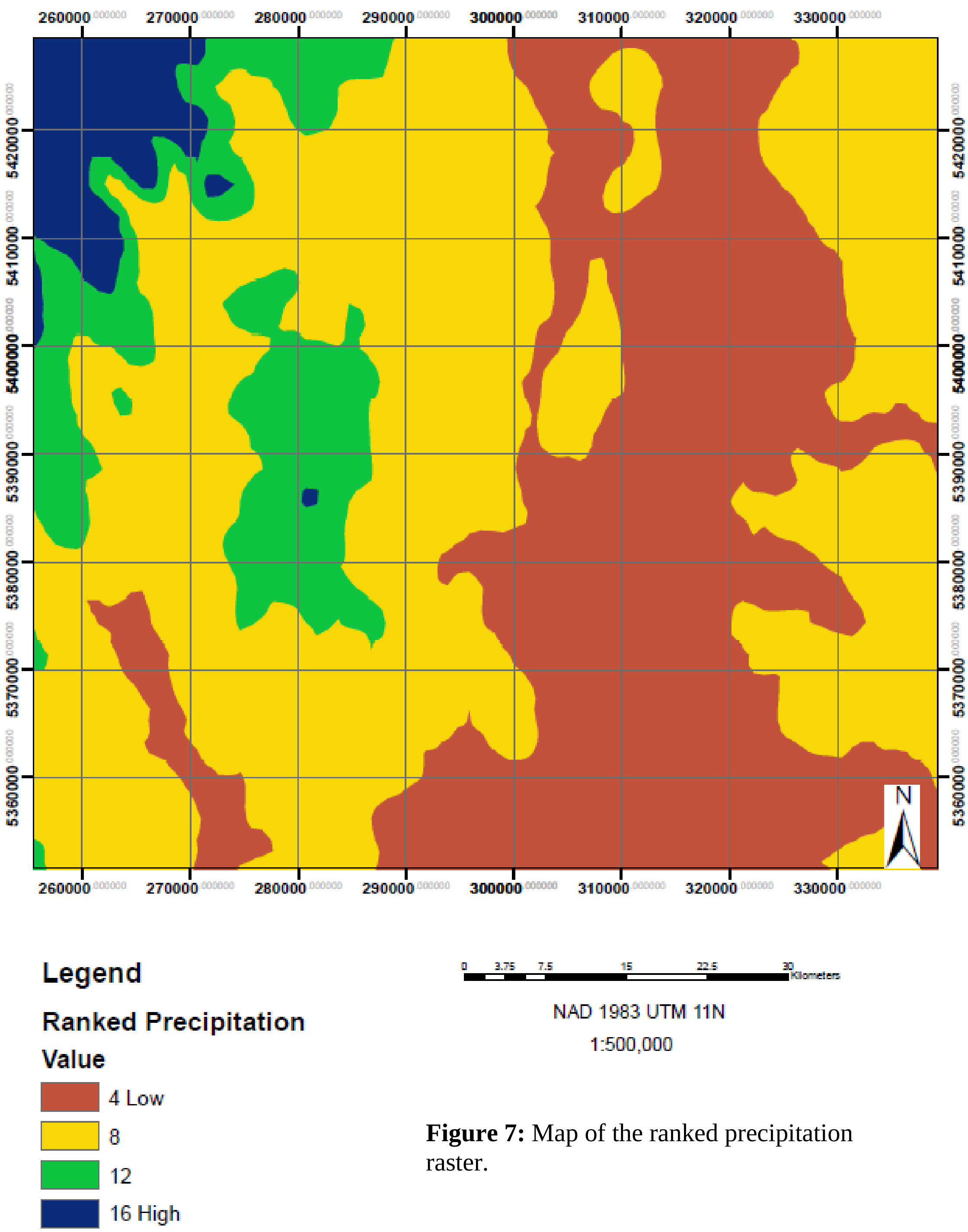

Figure 7: Map of the ranked precipitation raster.

The ranked precipitation raster was created using the clipped precipitation raster. The precipitation raster was reclassified with 242 to 400 mm, 400 to 700 mm, 700 to 1000 mm, and greater than 1000 mm, as 4, 8, 12, and 16, respectively. The final map is shown in Figure 7.

2.4 Creating the Erosion Susceptibility Raster

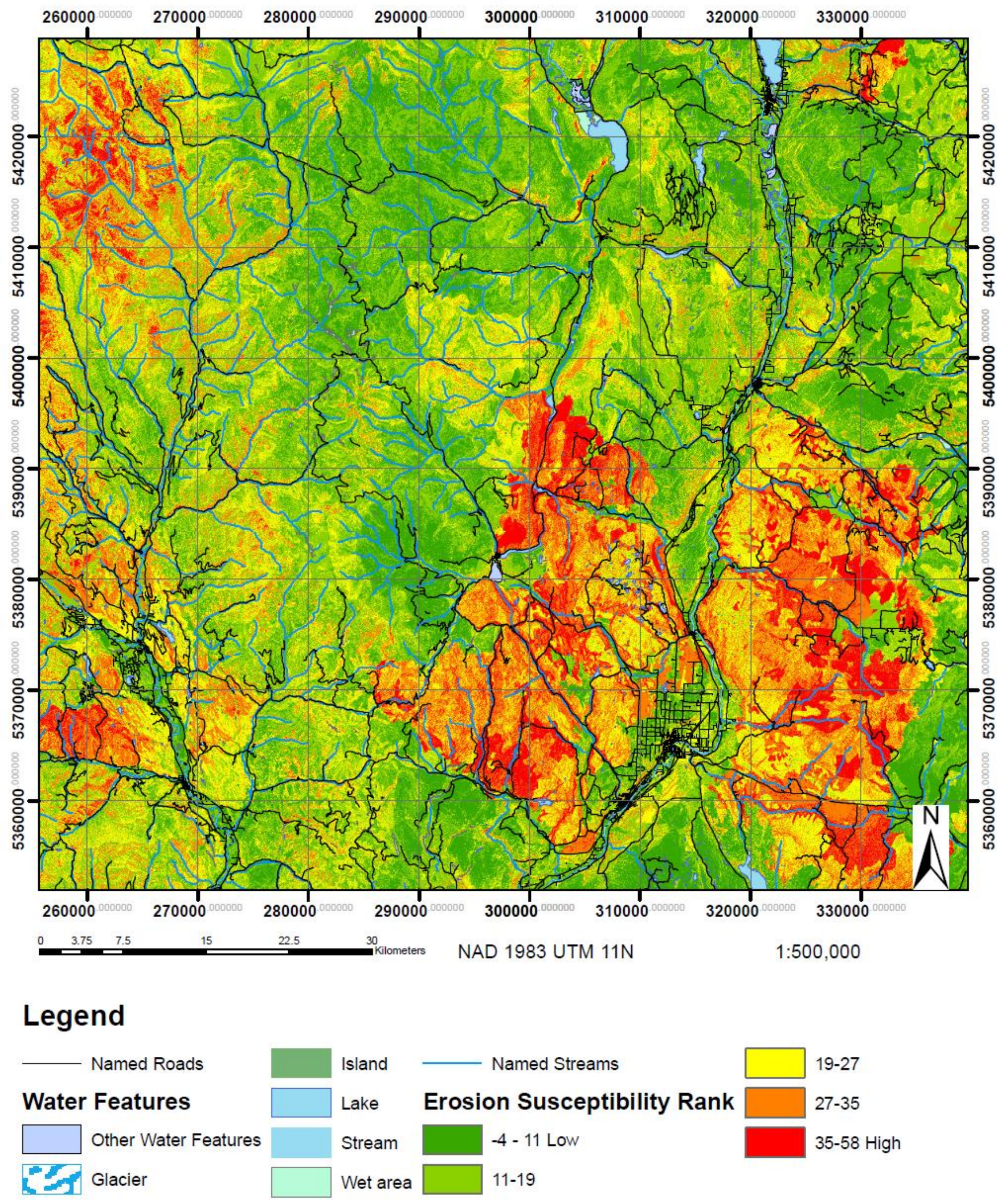

Figure 8: Erosion susceptibility map with roads and water features. Most susceptible areas are red and least susceptible are green.

The erosion susceptibility raster was created by using the map algebra tool. I added the lithology (Fig. 3), cover type (Fig. 5), slope (Fig. 6), and precipitation (Fig. 7) ranked rasters to calculate the erosion susceptibility raster (Fig. 8).

3. Results

When the erosion susceptibility map is compared to the fire map (Fig. 9) it is clear that there is a strong correlation between the burn area and some of the highest erosion susceptibilities.

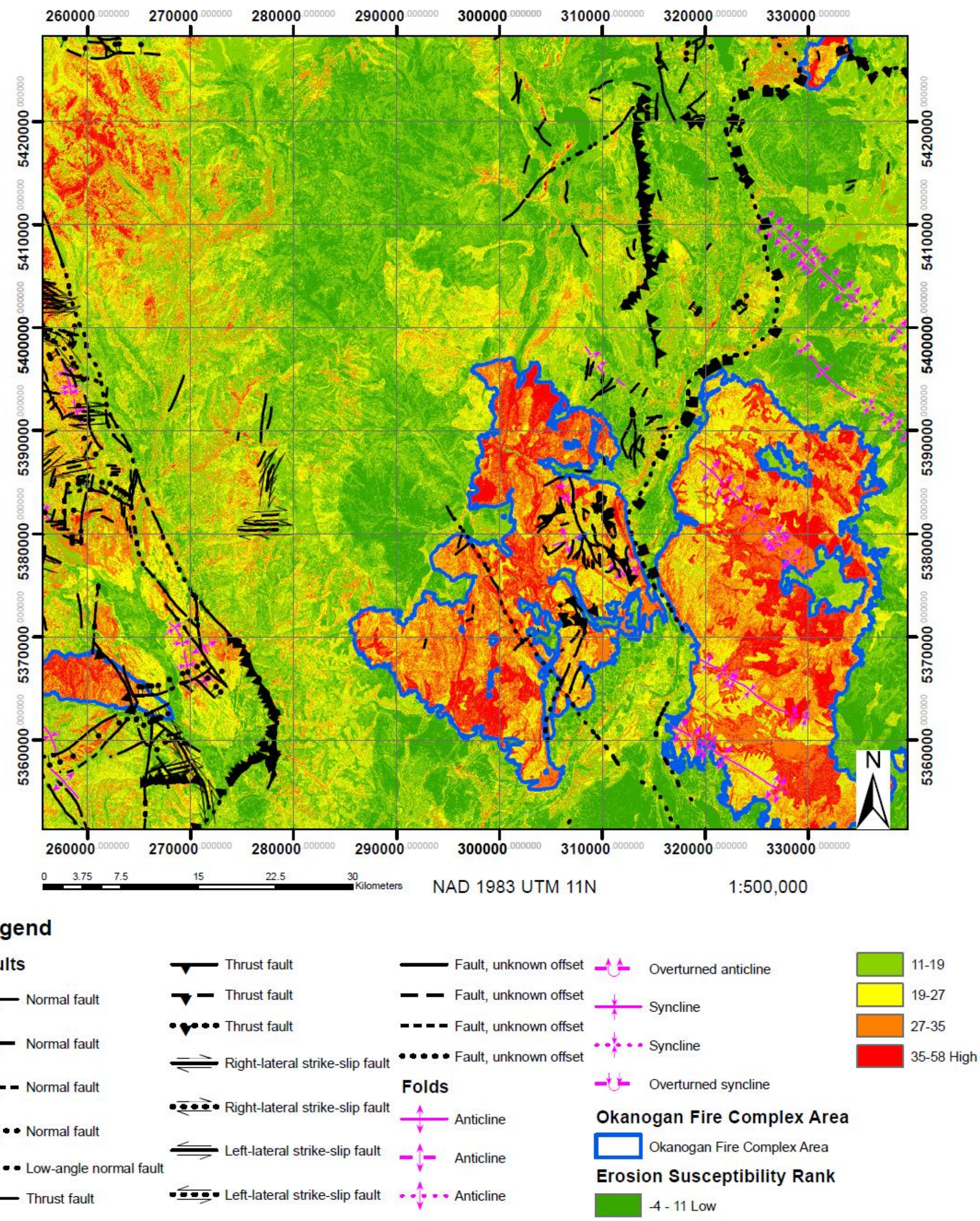

Figure 9: The erosion susceptibility map with structures and the fire area on top of the map.

However, there is also a region of high erosion susceptibility in the west and northwest quadrants of the map.

4. Discussion

Overall the areas most susceptible to erosion are ones affected by the fire, because the vegetation is no longer there to stabilize the sediment, and the effects of lithology weakness, precipitation amount, and slope angle become stronger. The northwestern region on the map also has high susceptibility ranks but is not associated with a burned region. This area is probably experiencing almost equal ranks of erosion susceptibility to burned areas because it is in an area with high precipitation, has some of the highest slopes, and has variable vegetation cover with large barren areas. All of these things combined explain why that region has such a high erosion susceptibility rank.

The western region also has high rates of erosion. This is most likely due to weaker lithologies, large areas of barren land, and slightly steeper slopes. It may also be correlated to structures, such as faults. In Lab 11, we calculated erosion susceptibility in Yellowstone National Park, and noticed a trend that erosion rates were lower in the caldera and erosion rates were slightly higher along faults. In Yellowstone, this relationship was most likely due to the caldera acting as a bowl, and thus, made it harder for sediment and rock to be eroded away. The faults most likely had higher rates of erosion because they were uplifting rock. Fault movement would increase slope, and steeper slopes would make it easier to erode material. This is likely why there is a correlation between faults and high erosion rates. However, the faults in Yellowstone were relatively recent and the faults in the western region are at the oldest postdate the Paleocene. This could have given more time to erode the rocks and decrease slopes, which could explain why there is a weaker correlation in this map than with Yellowstone’s erosion susceptibility map.

5. Conclusion

The fire area has the strongest correlation with erosion susceptibility, but other areas within the region also have high susceptibility rates. However, they are not as dangerous because they are further away from urban areas. From Figure 8, one can see that the urban area is bounded on two sides by high erosion susceptible areas. High erosion rates can destabilize hills and cause dangerous hazards, such as landslides. Considering this fire occurred in September 2015 just 9 months ago, it would be wise to revegetate the area in order to stabilize slopes.

6. References

Reubens, B., Posen, J., Danjon, F., Geudens, G., and Muys, B., 2007, The role of fie and coarse roots in shallow slope stability and soil erosion control with a focus on root system architecture: a review, Springer-Verlag, v. 21, p. 385-402

Sklar, L.S. and Dietrich, W.E., 2001, Sediment and rock strength controls on river incision into bedrock, Geological Society of America, v. 29, p. 1087-1090.